

# Influence of Precipitated Phase Formation on Recrystallization Behavior of Superalloy 718

Hwa-Teng Lee<sup>1,\*1</sup> and Wen-Hsin Hou<sup>1,2,\*2</sup>

<sup>1</sup>Department of Mechanical Engineering, National Cheng Kung University, No.1, University Road, Tainan 701, Taiwan, R. O. China

<sup>2</sup>Research & Development Center, Gloria Material Technology Corp., 35, Hsin Chung Road, Hsin Ying Dist, Tainan 730, Taiwan, R. O. China

Post heat treatment fails to refine the grain structure of superalloy 718. Thus, for components with demanding grain size requirements, the forging process should be performed within an extremely limited temperature region just below the  $\delta$  solvus temperature, yet higher than that required to induce dynamic recrystallization. The grain size of superalloy 718 is generally controlled during manufacturing by inducing full dynamic recrystallization through means of a carefully-controlled hot forming process performed in a powerful and precise forging machine. This work presents an alternative method for obtaining a fine and uniform grain structure through means of static recrystallization and a proper control of the  $\delta$  phase formation. In the proposed method, the component is cooled in water immediately after forging to suppress  $\delta$  phase precipitation and preserve the internal strain energy produced by the hot deformation process. The component is then heated to a temperature 30°C lower than the  $\delta$  solvus temperature 1030°C; resulting in a continuous recrystallization of the microstructure. Experimental results indicate that  $\gamma''$  phase precipitation and  $\delta$  phase precipitation dominate the dynamic and static recrystallization behaviors observed in the conventional and proposed grain refinement methods, respectively. Our results further demonstrate that the proposed static recrystallization method yields a fine microstructure with an average grain size of ASTM No. 7 (31.8  $\mu\text{m}$ ). Thus, the proposed method provides an inexpensive and technically straightforward alternative to the conventional hot forming grain refinement method. [doi:10.2320/matertrans.M2012090]

(Received March 7, 2012; Accepted May 1, 2012; Published June 20, 2012)

**Keywords:** static recrystallization,  $\delta$  phase, solvus, superalloy, fine grain

## 1. Introduction

Superalloy 718 is a widely used superalloy worldwide owing to its excellent mechanical properties and adequate corrosion resistance at a high temperature.<sup>1)</sup> The strength of superalloy 718 derives predominantly from metastable body centered tetragonal coherent  $\gamma''$  ( $\text{Ni}_3\text{Nb}$ ) precipitates in the matrix. However, the performance of superalloy 718 is highly sensitive to the grain size and microstructural uniformity. In general, the grain size produced with conventional procedure is by ASTM grain size 4.5–6.<sup>2)</sup>

Park *et al.*<sup>3)</sup> found that the austenitic structure of superalloy 718 prevents the use of traditional heat treatment processes in reducing the grain size. Similarly, Camus *et al.*<sup>4)</sup> showed that the un-recrystallized grains in the microstructure of hot-worked superalloy 718 components may not fully recrystallize when subjected to further thermal deformation. Consequently, dynamic or meta-dynamic recrystallization has attracted significant attention as an effective means of producing superalloy 718 components with a fine and evenly-distributed grain structure during hot forming processes.<sup>5–9)</sup> Moreover, Thermomechanical Process would achieve finer grain structure by aging and precipitation of a high volume fraction of acicular  $\delta$  phase before hot forming and during the subsequent dynamic recrystallization process; the  $\delta$  phase inhibits recrystallized grain growth and generate a grain finer than ASTM No. 10.<sup>10)</sup> However, even slight deviations of the forging temperature from the designed value may significantly change the microstructure. For instance, lower-temperature areas of the forging commonly retain un-

recrystallized grains of the original billet.<sup>11)</sup> The initial grain size of superalloy 718 components depends on the finished forging temperature. Producing a fine grain structure requires a deformation temperature lower than the  $\delta$  solvus temperature. However, while a lower deformation temperature is beneficial in reducing the grain size, it also prompts a reduction in the volume fraction of recrystallized grains.<sup>12)</sup> Therefore, in practice, adequately controlling the grain size of superalloy 718 components is extremely challenging, and is only possible with the assistance of a highly effective, precisely-controlled hot forging system.

While pertinent literature contains various proposals for refining the grain size of superalloy 718 via dynamic recrystallization, the feasibility of using static recrystallization as a refinement mechanism has seldom been examined. Therefore, this work presents a novel recrystallized method for refining the grain structure of superalloy 718 through means of static recrystallization and adequate control of the  $\delta$  phase formation within the austenitic microstructure. In the proposed method, the component is cooled in water immediately after forging to suppress  $\delta$  phase precipitation, followed by heating to a temperature immediately below the  $\delta$  solvus temperature, resulting in continuous recrystallization of the microstructure. The present results obtained by proposed procedure indicate that recrystallization is not induced exclusively by hot forming, as widely claimed in the literature. The technique proposed provides a feasible controlling over the grain size without an energy consumptive and technically sophisticated hot forming process.

Next, the refined microstructure is characterized using optical microscopy (OM), scanning electron microscopy (SEM), transmission electron microscopy (TEM) and ultra-high resolution analytical electron microscopy (HRAEM).

\*1Corresponding author, E-mail: htlee@mail.ncku.edu.tw

\*2Graduate Student, National Cheng Kung University

Table 1 Chemical composition of Superalloy 718 (unit: mass%, Fe: balance).

Item	C	Si	Mn	P	S	Ni	Cr	Mo	Cu
AMS5662									
Min						50.00	17.00	2.80	
Max.	0.08	0.35	0.35	0.015	0.015	55.00	21.00	3.30	0.30
Value	0.05	0.08	0.03	0.006	0.001	52.29	18.34	3.12	0.02
Item	Al	Co	Ti	B	Nb	Ta	Pb	Bi	Se
AMS5662									
Min	0.20		0.65		4.75				
Max.	0.80	1.00	1.15	0.006	5.50	0.05	0.005	0.00003	0.0003
Value	0.54	0.13	0.97	0.004	5.15	0.03	0.0000(1)	0.00001	0.0000(4)

Additionally, the precipitation mechanisms governing the dynamic and static recrystallization behaviors observed in the conventional superalloy 718 refinement procedures and the proposed refinement method are compared.

## 2. Experimental Section

### 2.1 Materials

Table 1 lists the composition of the Superalloy 718 used in this work. Superalloy 718 ingots with a diameter of 480 mm were fabricated via vacuum induction melting (VIM), followed by vacuum arc remelting (VAR). A standard homogenization treatment was then performed before an open-die pre-forging procedure designed to reduce the ingot diameter to 350 mm. A final forging procedure was then implemented using a four-hammer precision forging machine to reduce the circular ingot to a square bar with dimensions of 133 mm × 133 mm.

The pre-heating temperature for the original ingots and the pre-forged bars was set to 1130°C to ensure the complete dissolution of the  $\delta$  phase into the matrix before hot working. The volume fraction of recrystallized grains in superalloy 718 generally depends on the temperature, strain and strain rate. Also, a higher fraction of un-recrystallized grains normally occurs at a low temperature.<sup>13)</sup> Therefore, the final forging procedure was performed at a comparatively low temperature of 950°C and was followed immediately by a water quenching process to maintain the un-recrystallized microstructure.

### 2.2 Heat treatment

Three heat treatment procedures were performed. First, as-forged samples were recrystallized at temperatures ranging from 950–1030°C for 1 h and then quenched in water to investigate how heat treatment temperature affects the static recrystallization results. Additionally, exactly how heat treatment temperature and holding time affect the static recrystallization effect was investigated by heat treating as-forged samples at temperatures ranging from 990–1010°C for 2.5–60 min and, then, quenching the samples immediately in water. Moreover, exactly how large-scale  $\delta$  phase precipitation affects the static recrystallization behavior of superalloy 718 was investigated by ageing as-forged specimens at 910°C for 5 h, heat treatment at a temperature of 1000°C for 60–135 min and, then, quenching in water.

### 2.3 Quantitative metallography

The extent of  $\delta$  phase precipitation within various samples was examined quantitatively via SEM analysis. Before analyses were performed, preliminary observations were made to check the uniformity of  $\delta$  phase distribution and identify the most appropriate magnification conditions, under which, to observe and compare different samples. According to our results, a magnification of 1500 times yielded the optimum compromise between  $\delta$  phase and matrix structure. Owing to the large number of samples under observation, just 10 images were acquired for each sample, in which the samples were taken at regular intervals along the central axis of the section containing the highest number of precipitates. Finally, the  $\delta$  phase content in each image was analyzed using a Leica image analyzer.

### 2.4 Metallographic preparation

Specimens for optical microscopy were prepared via mechanical polishing, followed by chemical etching using a swab containing a solution of 20 g CuCl<sub>2</sub> (copper chloride), 200 ml HCl (hydrochloric acid) and 200 ml CH<sub>3</sub>OH (methanol). Thin foil samples for TEM observations were then prepared using a dual jet electro-polishing machine with an electrolyte consisting of 10 vol% hydrochloric acid, 30 vol% 1-butanol and 60 vol% ethanol. Next, the samples were polished using an agitation voltage of 20 V and an electrolyte temperature of −25°C. Notably, preparing TEM samples of the unrecrystallized structure using this electro-polishing method is extremely difficult since the electro-polishing location can not be controlled precisely as the focused ion beam (FIB) can. Therefore, samples of the unrecrystallized structure were prepared using a FIB method.

The above samples were observed using an optical microscope, ultrahigh resolution analytical electron microscope (HRAEM- Jeol JEM-2100F CS STEM), and field emission scanning electron microscope (FE-SEM) equipped with an energy-dispersive X-ray spectroscope (EDS).

## 3. Results and Discussion

### 3.1 Observations of as-forged microstructure

Figure 1(a) presents an OM micrograph of a typical as-forged superalloy 718 sample. As expected, the microstructure contains several coarse un-recrystallized grains, owing to the relatively low temperature used in forging

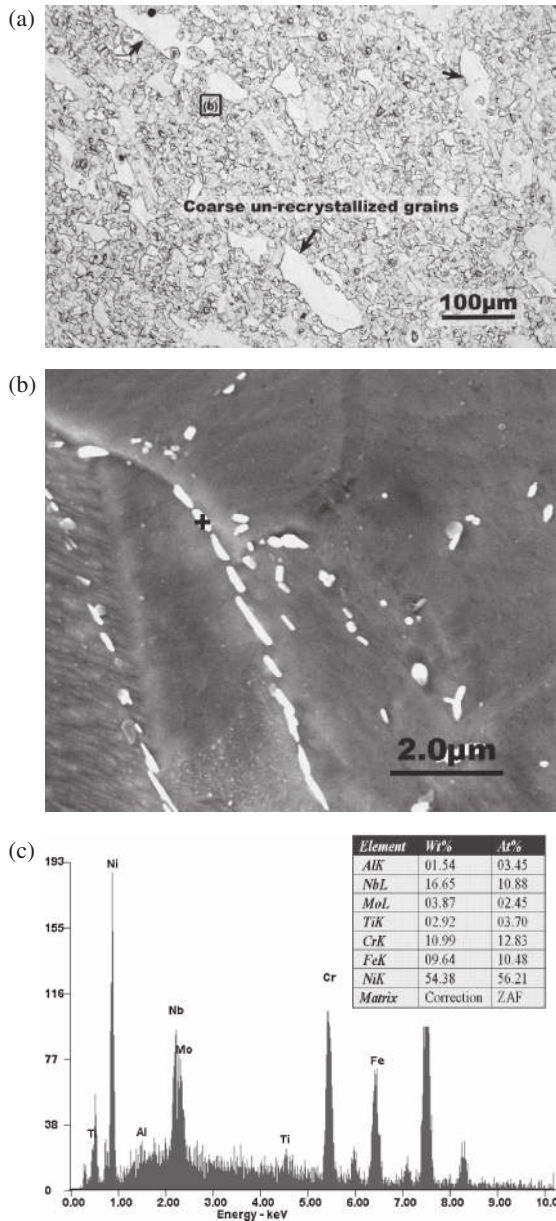


Fig. 1 As-forged microstructure of superalloy 718 superalloy and precipitation composition: (a) coarse un-recrystallized grains within as-forged microstructure (denoted by arrows); (b) accumulation of  $\delta$  phase precipitates at grain boundary (Notably, the micrograph corresponds to the square in (a)); and (c) EDS analysis results showing precipitates to be Nb-enriched phase.

(950°C). Figure 1(b) shows an FE-SEM image of the microstructure within the area bounded by the purplish square in Fig. 1(a). Closely examining this image reveals that the volume fraction of precipitation is around 1.2% and the largest precipitates have a length of approximately 2  $\mu\text{m}$ . EDS analysis results shown in Fig. 1(c) indicate that the precipitates contain 56.2 at% Ni and 10.9 at% Nb. Since the matrix contains 48.0 at% Ni and 4.0 at% Nb, EDS results indicate that the precipitates are niobium-enriched phase.

Figure 2(a) presents a TEM micrograph of the dynamic recrystallization microstructure of a superalloy 718 specimen forged at 950°C and, then, quenched immediately in water. This figure reveals that the microstructure contains a few dislocations, which are caused by stress generated during

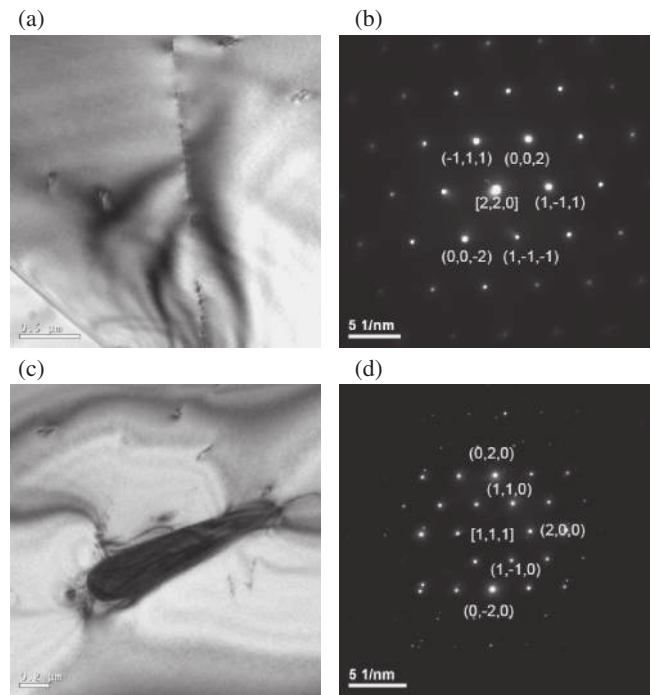


Fig. 2 TEM bright field images and diffraction patterns: (a) matrix containing dislocations; (b) diffraction pattern corresponding to the matrix; (c) needle-shaped precipitates in matrix; (d) diffraction pattern showing precipitates to be  $\delta$  phase.

quenching. The diffraction pattern in Fig. 2(b) indicates that the matrix contains only a single phase, while the TEM image in Fig. 2(c) shows the rod-like precipitate. Finally, according to the selected area diffraction (SAD) pattern in Fig. 2(d), the phase is  $\delta$  phase.

According to Sundararaman *et al.*,<sup>14,15)</sup> superalloy 718 exhibits two forms of  $\delta$  phase precipitation, i.e., (1) heterogeneous precipitation at the grain and twin boundaries, followed by the growth of thin plates into the grains, and (2) intragranular precipitation, often initiated by stacking faults located within pre-existing  $\gamma'$  precipitates. The micrograph in Fig. 1(b) shows rod-like  $\delta$  phase precipitates at the grain boundaries (i.e., the first form of  $\delta$  phase precipitation described in Refs. 14, 15)).

In the present experiments, the total elapsed time between retrieving the pre-forged ingots from the pre-heating furnace and the end of the final forging process was less than 15 min. Therefore, we conclude that the rate of  $\delta$  phase precipitation during the forging process is more rapid than that in a strain-free process, resulting in the formation of  $\delta$  phase with increasing strain energy.<sup>16-18)</sup>

Figure 3 displays a TEM micrograph of the un-recrystallized structure of as-forged and water cooling sample. This figure reveals that the structure has a mottled appearance and significantly differs from the dynamic recrystallization matrix shown in Fig. 2. As is generally assumed, the mottled appearance originates from misfit strains due to matrix-precipitate disregistry and an interaction of the strain fields associated with different precipitate variants. Thus, the mottled appearance implies that the matrix contains fine, ordered particles caused by a short holding time and high temperature; these particles may started to form at this

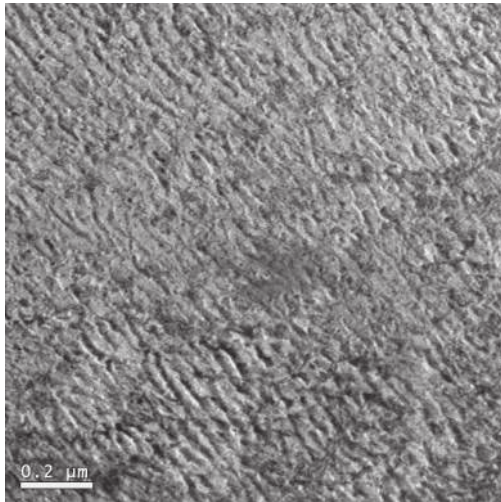


Fig. 3 TEM bright field image of unrecrystallized structure of as-forged specimen.

stage.<sup>19)</sup> However, these particles are too fine for clear discernment in the TEM micrograph.

Particles in the un-recrystallized structure of the sample were examined more clearly using HRAEM. The HRAEM micrograph in Fig. 4(a) indicates that the un-recrystallized structure contains two precipitate morphologies, i.e., circular plate-shaped (Label 1, less easily discerned) and lens-shaped (Label 2, easily discerned). The SAD pattern in Fig. 4(b) reveals the presence of superlattice reflection, implying the precipitation of coherent phases within the matrix. The dark field images in Figs. 4(c) and 4(d) display clear pictures of the matrix and particles, respectively. Figures 4(e) and 4(f) illustrate the nano-beam diffraction patterns (NBDPs) in the [110] matrix zone axis of the two particles in Fig. 4(a). Additionally, the SAD pattern in the [110] plane was simulated using computer software. According to those results, the two particles were [021] and [201]  $\gamma''$  phase, respectively.<sup>20)</sup>

Here, the finish forging temperature was controlled at a relatively low temperature of 950°C. Notably, this temperature exceeds the  $\gamma''$  solvus temperature, i.e., 915°C.<sup>21)</sup> However, the  $\gamma''$  phase that precipitated this finding correlates well with the findings of Ref. 17) in which dynamic precipitation accelerates the precipitation kinetics and likely moves higher temperatures up the static precipitation time temperature (PTT) diagram.

Particles, especially if closely spaced, exert a significant pinning effect on the low and high angle grain boundaries, and, therefore, inhibit recrystallization.<sup>22)</sup> Nickel alloys contain weak equiaxed coherent particles, which deform at the same rate as the matrix, and exhibit retarded recrystallization.<sup>23)</sup> Therefore, the unrecrystallized structure in the as forged specimen in Fig. 4(a) implies that the strain energy produced during low temperature deformation induces the precipitation of coherent  $\gamma''$  phase which retards dynamic recrystallization.

### 3.2 Effect of post heat treatment on static recrystallization

The as-forged samples were solution heat treated at temperatures of 950, 980, 1000 and 1030°C for 1 h and,

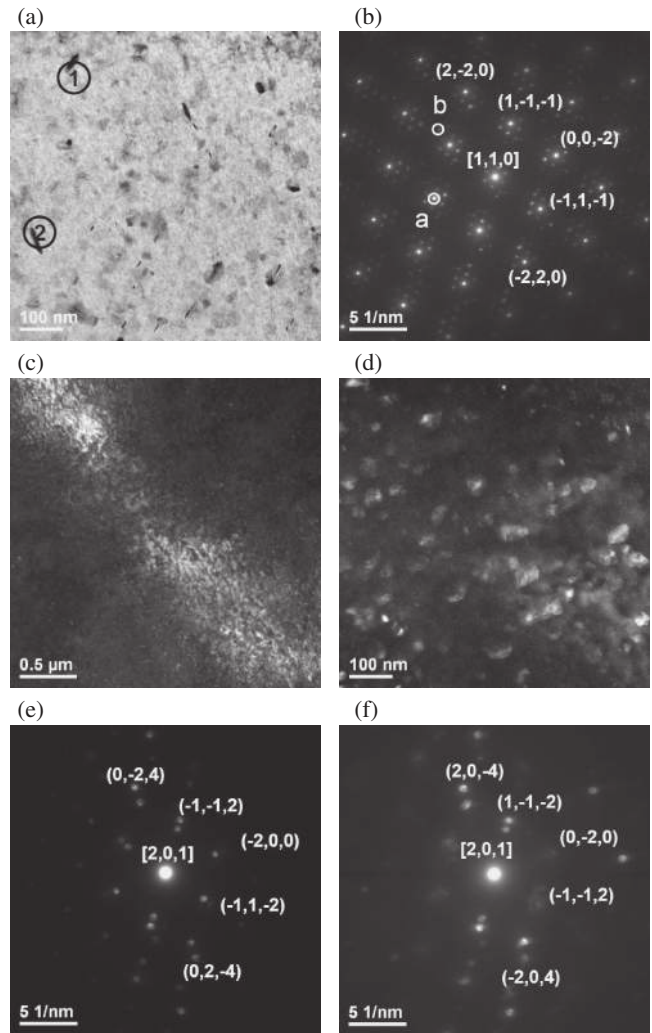


Fig. 4 HRAEM bright field images and diffraction patterns of unrecrystallized structure: (a) matrix containing very fine precipitates; (b) diffraction pattern corresponding to the matrix; (c) dark field image corresponding to reflection point (a) in (b); (d) dark field image corresponding to reflection point (b) in (b); (e) narrow beam diffraction pattern corresponding to location 1 in (a); and (f) narrow beam diffraction pattern corresponding to location 2 in (a).

then, were quenched in water. Figure 5(a) illustrates the recrystallization states of the as-forged sample and the four heat-treated samples. Figure 5(b) indicates that the grain size distribution within various conditions.

According to Fig. 5(a), the as-forged specimen and the specimens heat treated at 950 and 980°C, respectively, contain un-recrystallized coarse grains in the microstructure and an accumulation of  $\delta$  phase precipitates at the grain boundaries. However, for the samples solution heat treated at higher temperatures of 1000 or 1030°C, the  $\delta$  phase dissolves fully into the matrix; subsequently producing a clean, precipitate-free grain boundary and a uniform grain structure.

Figure 5(a) further demonstrates that the volume fraction of  $\delta$  phase varies according to the temperature applied during the solution heat treatment. For instance, the volume fraction of  $\delta$  phase in the as-forged sample equals 1.2%, yet increases to 3.4% in the sample heat treated at 950°C. When the heat treatment temperature is increased to 980°C, the volume fraction falls to around 1.4%. Finally, when the heat

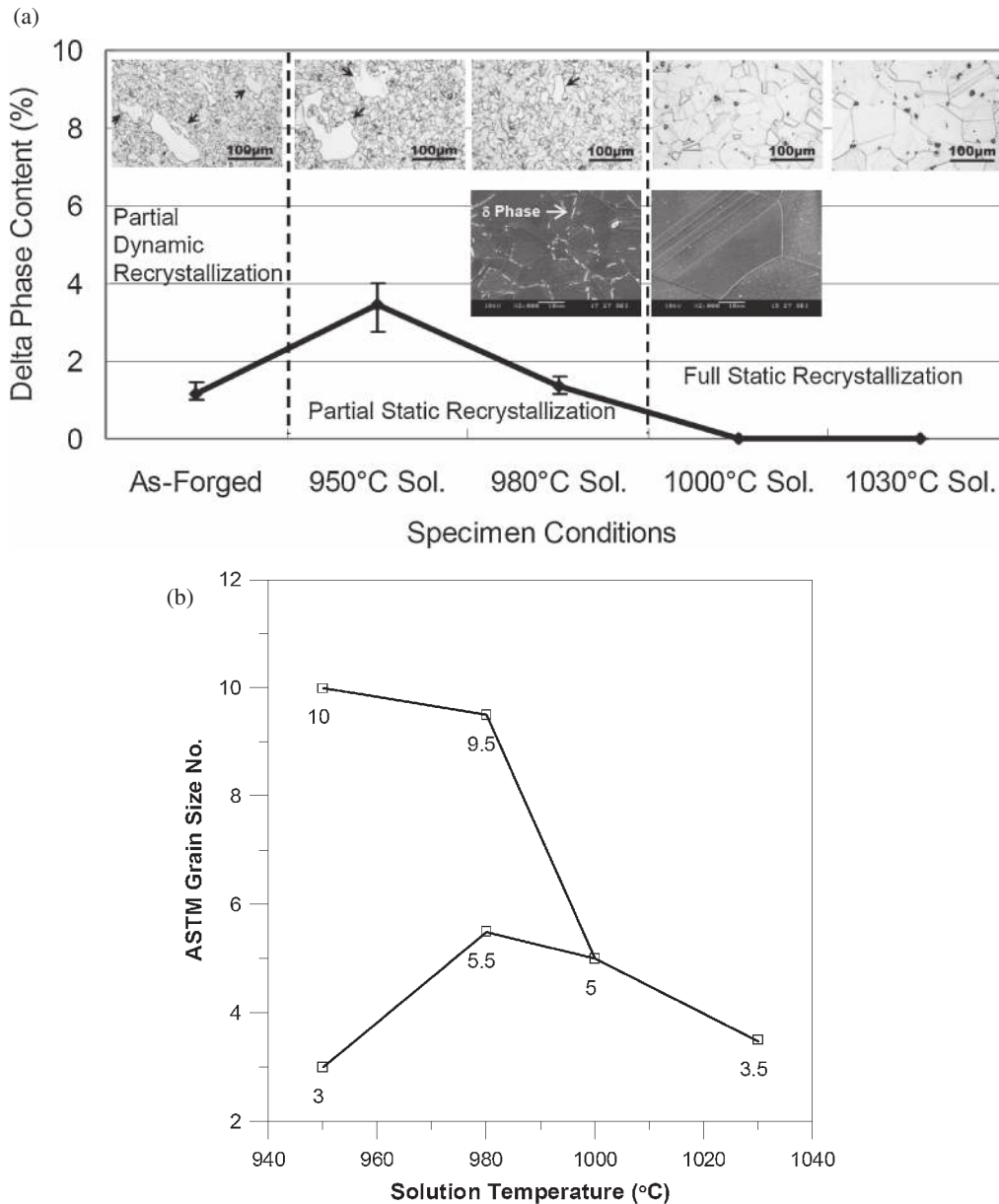


Fig. 5 Grain size characteristics and extent of recrystallization in as-forged and solution heat-treated superalloy 718 samples: (a) OM grain structure at various conditions; (b) grain size distribution.

treatment temperature is increased to 1000°C or higher, the volume fraction reduces to virtually zero. Additionally, the  $\delta$  phase precipitates exert a pinning effect at the grain boundaries, thus inhibiting recovery and recrystallization.<sup>22)</sup> However, increases the heat treatment temperature dissolves the  $\delta$  phase, leading to full static recrystallization.

According to Fig. 5,  $\delta$  phase in the superalloy 718 microstructure plays a major role in determining the extent of recrystallization. Thus, in the proposed static recrystallization method, the samples are quenched in water immediately after forging to suppress  $\delta$  phase precipitation. This figure also reveals that heat treating as-forged superalloy 718 components at a temperature sufficiently high to dissolve  $\delta$  phase precipitation in the matrix can produce a fine homogeneous austenitic grain structure. Importantly, above results demonstrate that recrystallization is not induced exclusively by hot forming, as widely claimed in the literature.<sup>3)</sup>

### 3.3 Effect of heat treatment temperature and holding time on static recrystallization

This work also investigates how heat treatment temperature and holding time affect the static recrystallization effect by solution heat treatment of as-forged superalloy 718 samples at temperatures of 990, 1000 and 1010°C for between 2.5 and 60 min and, then, quenching them immediately in water. Figure 6 describes the OM microstructures and the grain distribution of the various samples. For the sample heat treated at 990°C for 10 min, the grain size conforms to that defined in ASTM No. 8 (i.e., 22.5  $\mu$ m). However, increasing the holding time increases the grain size and causes abnormal grain growth heterogeneously throughout the microstructure. Consequently, the microstructure transforms to a duplex structure.

The SEM micrograph in Fig. 7 reveals that the fine grain boundaries in the sample heat treated at 990°C for 30 min

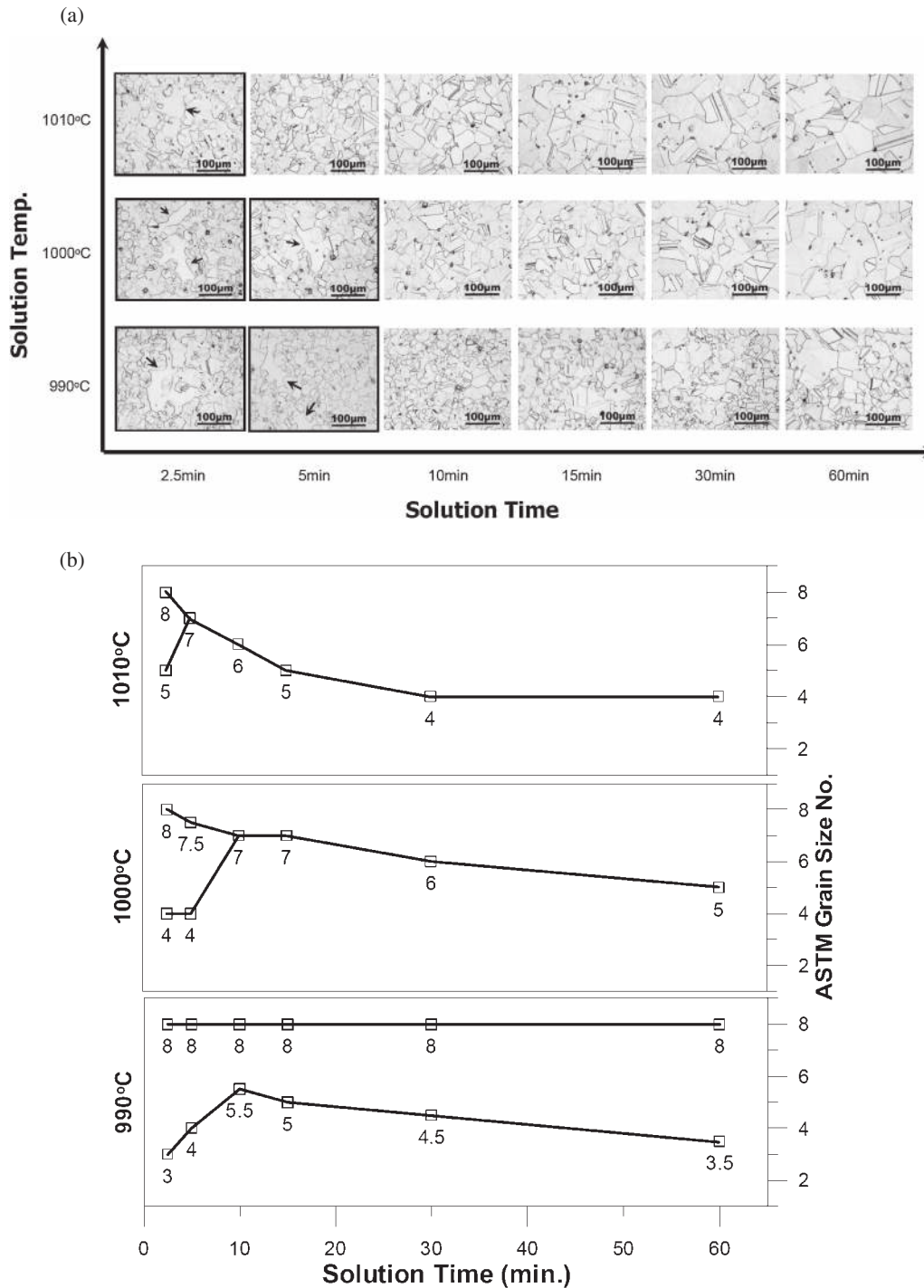


Fig. 6 Recrystallization process in forged superalloy 718 samples solution heat treated at temperatures of 990, 1000 and 1010°C for 2.5–60 min: (a) OM grain structure under various conditions; (b) grain size distribution.

are surrounded by fine  $\delta$  phase precipitates, which pin the grain boundary and prevent grain growth. However, the coarse grain boundaries contain no  $\delta$  phase and, thus, their growth is unimpeded. According to this figure, the duplex structure of the samples heat treated at a temperature of 990°C for 30 min or longer is owing to heterogeneous  $\delta$  phase precipitation.

In practice, the strain energy induced in the forging of superalloy 718 facilitates and modifies the precipitation behavior of  $\delta$  phase.<sup>24)</sup> Since forging causes anisotropic deformation, the residual strain energy is non-uniformly

distributed. Consequently, a non-homogeneous precipitation of  $\delta$  phase occurs, thus leading to the evolution of a duplex structure in the subsequent heat treatment.

Figure 6 shows the OM results and grain size distribution for the sample heat treated at a temperature of 1000°C, indicating that full static recrystallization occurs after approximately 10 min. The resulting grain size corresponds to that of ASTM No. 7 (i.e., 31.8  $\mu\text{m}$ ). However, the grain size increases with an increasing heating time. Thus, after 60 min, the grains have a size of around 63.5  $\mu\text{m}$ , which corresponds to ASTM No. 5. Notably, the heat treated

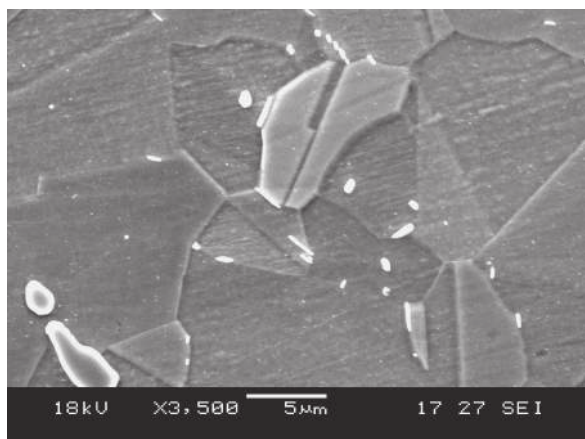


Fig. 7 SEM micrograph showing an accumulation of fine  $\delta$  phase precipitates at the fine grain boundaries of the sample heat treated at 990°C for 30 min.

microstructures have a uniform grain size, suggesting that grain growth occurs continuously and is unimpeded by the  $\delta$  phase at the grain boundaries. For the highest heat treatment temperature of 1010°C, a full static recrystallization of the superalloy 718 microstructure occurs after 5 min (upper row of Fig. 6(a)). The grain size correlates with that of ASTM No. 7 (i.e., 31.8  $\mu\text{m}$ ). However, the grain size increases rapidly when increasing the holding time. Thus, a grain size consistent with that of ASTM No. 5 is obtained after only 15 min.

Above results confirm that the original coarse un-recrystallized grains in the as-forged superalloy 718 specimen can be refined to a grain size consistent with that of ASTM No. 7 via a static recrystallization approach induced by adequately controlling the temperature and the holding time. However, at temperatures of 1000°C or higher, full static recrystallization occurs after 5–10 min, and the grain size increases uniformly when increasing the holding time.

### 3.4 Effect of large-scale $\delta$ phase precipitation on static recrystallization

Exactly how large-scale  $\delta$  phase precipitation affects the static recrystallization of superalloy 718 was investigated by ageing as-forged specimens at 910°C for 5 h, subsequently forming a large number of rod-like  $\delta$  phase precipitates at the grain boundaries and within the grains themselves (Fig. 8). Closely examining the aged samples reveals that the volume fraction of  $\delta$  phase increased from 1.2% in the as-forged sample to approximately 16% following the ageing process. The aged samples were further heat treated at a temperature of 1000°C from 60 to 135 min and, then, quenched immediately in water. In Fig. 9(a), corresponding to an ageing time of 60 min, the rod-like  $\delta$  phases are partially dissolved into the matrix and have a breakage appearance. Moreover, the dissolution breakage  $\delta$  phase is obvious in the unrecrystallized grains and at the grain boundaries. For an extended holding time of 135 min, Fig. 9(b) indicates that the sample has a bimodal microstructure consisting mainly of fine grains (ASTM No. 10) and a small number of coarser grains. Furthermore, according to Fig. 9(c), the duplex microstructure contains the residual rod-like  $\delta$  phase.

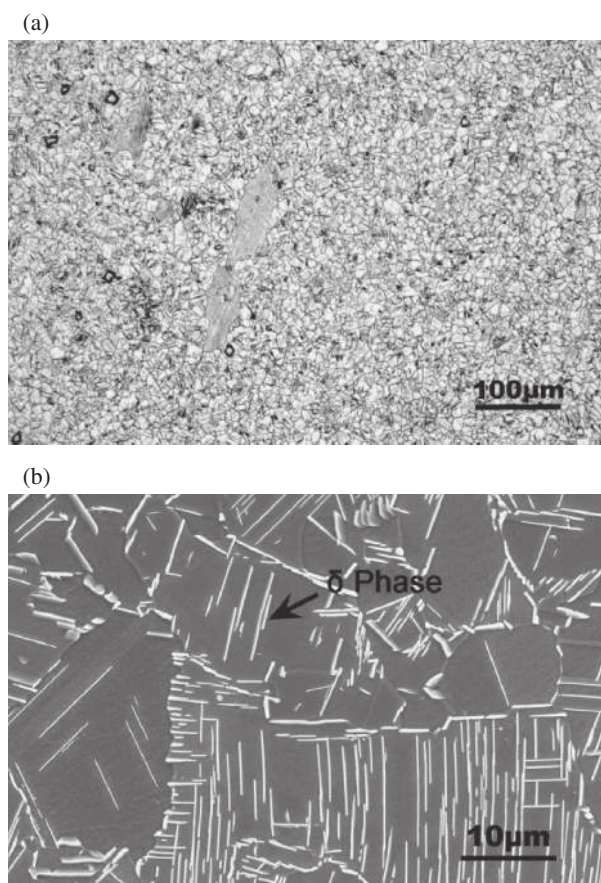


Fig. 8 SEM micrographs of as-forged specimen aged at 910°C for 5 h: (a) precipitation of large number of  $\delta$  phase precipitates; (b) enlarged SEM image of  $\delta$  phase.

For superalloy 718, the microstructure developed during recrystallization depends on the distribution of the undissolved  $\delta$  phase precipitates. Solution behavior of the precipitated  $\delta$  phase subsequently depends on the Nb segregation within the microstructure. During solidification, the primary dendrites reject Nb into the interdendritic liquid and the resulting low-Nb dendrites grow into solidifying metal in a direction perpendicular to the solidification front. According to the literature,<sup>11)</sup> the nominal Nb content of superalloy 718 is around 5 mass%. Moreover, the primary dendrite structure nominally contains 3 mass% Nb, while the interdendritic region nominally contains around 9 mass% Nb. Therefore, a Nb-enriched eutectic region is generally found between the dendrites within the casting grain of superalloy 718 ingots. However, the above structure can be improved via prolonged homogenization treatment.<sup>25)</sup> The dissolution temperature of  $\delta$  phase in superalloy 718 increases with an increasing Nb content.<sup>26)</sup> Consequently, the  $\delta$  solvus temperature varies from one location of the microstructure to another, according to Nb-rich and Nb-lean regions, respectively.<sup>10)</sup> Given a large number of  $\delta$  phase precipitates and a heat treatment temperature of 1000°C (i.e., lower than, yet close to the average  $\delta$  solvus value), the  $\delta$  phase fails to dissolve thoroughly into the matrix. Consequently, in the as-forged specimens aged at 910°C for 5 h and then solution heat treated at 1000°C for 135 min, the grains in the Nb-lean regions of the matrix (i.e., the regions in which the  $\delta$  phase is

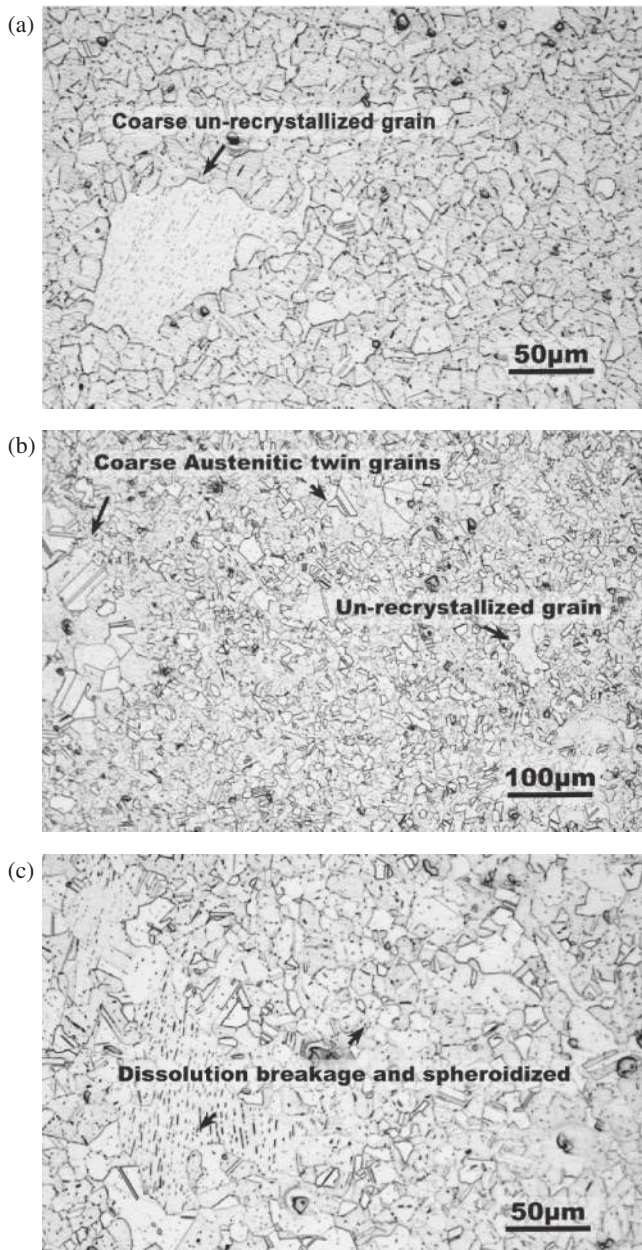


Fig. 9 OM micrographs of as-forged specimens aged at 910°C for 5 h and then solution heat treated at 1000°C for 60 or 135 min: (a) residual un-recrystallized coarse grains in specimen heat treated for 60 min; (b) bimodal structure produced by solution heat treatment for 135 min; and (c) residual rod-like  $\delta$  phase within un-recrystallized coarse grains.

fully dissolved) become recrystallized and grow in size, while those in the Nb-rich regions (i.e., the regions in which residual  $\delta$  phase remains) retain their original (fine) size and un-recrystallized structure (Fig. 9(b)). Notably, this finding markedly differs from that found in the as-forged samples containing a small number of  $\delta$  phase precipitates, in which the  $\delta$  phase dissolves completely into the matrix at a temperature of 1000°C, resulting in uniform full static recrystallization almost immediately (Fig. 5).

This work also simulated the characteristics of  $\delta$  precipitation and dissolution by using JMatPro software. Simulation results indicated that the maximum volume fraction of stable precipitates simulated by the chemical composition of the studied sample was around 14%, yet

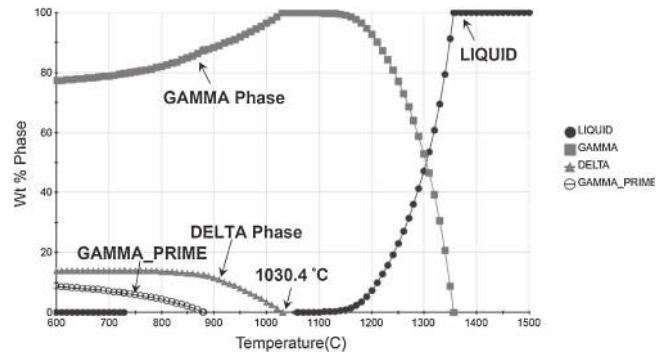


Fig. 10 JMatPro results showing  $\delta$  solvus temperature to be 1030.4°C.

decreased to 0% when increasing the heat treatment temperature to around 1030°C or higher. Moreover, the solvus temperature of the  $\delta$  phase was calculated to be 1030.4°C (Fig. 10). Notably, this temperature corresponds to that of Stockinger *et al.*<sup>27)</sup> At temperatures exceeding 980°C,  $\delta$  phase dissolution breakage occurs, resulting in the formation of spheroidized  $\delta$  phase precipitates.<sup>26)</sup> The  $\delta$  phase is distributed heterogeneously, resulting in the formation of a bimodal structure. As mentioned in Sections 3.2 and 3.4, the temperature required to achieve a full dissolution of the  $\delta$  phase into the matrix depends on the initial volume fraction of  $\delta$  phase in the microstructure. For samples with a large volume fraction of 16%  $\delta$  phase, a temperature of 1030°C or higher is required to achieve full recrystallization. However, a higher recrystallization temperature implies a larger grain size.

As mentioned earlier, the duplex microstructure is a direct consequence of heterogeneous  $\delta$  phase precipitation. In the proposed grain refinement method, rapid cooling in water following forging suppress the precipitation and growth of  $\delta$  phase. Consequently, the  $\delta$  phase has the form of minute spheroidized particles, which are fully dissolved into the matrix at a temperature of 1000°C (i.e., lower than the  $\delta$  solvus temperature) and lead to a continuous recrystallization of the microstructure, resulting in the formation of a fine grain size.

#### 4. Conclusions

This work has developed a novel recrystallized method for obtaining a fine and uniform grain structure in forged superalloy 718 components through means of a static recrystallization process and adequate control of the  $\delta$  phase formation. Based on the experimental results, we conclude the following:

- (1) Dynamic precipitation accelerates the precipitation kinetics. The resulting  $\gamma''$  coherent phase exerts a significant pinning effect on both high and low angle boundaries. Thus, in dynamic recrystallization, recrystallization kinetics is determined largely by fine particles dispersion, thus preventing recrystallization and resulting in an un-recrystallized structure at low hot forming temperatures.
- (2) In forged components containing a small volume fraction of the  $\delta$  phase, static recrystallization at



temperatures lower than 1000°C (i.e., between 980 and 1000°C) is suppressed since the  $\delta$  phase precipitates exert a significant pinning effect on the grain boundaries. The  $\delta$  phase precipitates are distributed heterogeneously within the microstructure, leading to a situation in which a duplex microstructure evolves when increasing the ageing time.

- (3) In forged components in which the  $\delta$  phase is constrained by water quenching to a volume fraction less than 1.2% and a length less than 2  $\mu\text{m}$ , full static recrystallization can be achieved at a temperature of 1000°C (i.e., 30°C lower than the  $\delta$  solvus temperature). The resulting microstructure contains equiaxed fine grains with an average size of 31.8  $\mu\text{m}$  (i.e., ASTM No. 7).
- (4) In superalloy 718 samples containing a large volume fraction of  $\delta$  phase precipitates, the  $\delta$  solvus temperature varies from one location to another owing to Nb segregation effects. Under such conditions, a heat treatment temperature close to (but lower than) the  $\delta$  solvus temperature fails to produce a fine and uniform grain structure.

#### Acknowledgements

The financial support provided to this study by the ITRI South, Industrial Technology Research Institute, Taiwan, Republic of China under Grant No. 9301XSY732 is gratefully acknowledged.

#### REFERENCES

- 1) S. H. Fu, J. X. Dong, M. C. Zhang and X. S. Xie: *Mater. Sci. Eng. A* **499** (2009) 215–220.
- 2) L. A. Jackman, G. J. Smith, A. W. Dix and M. L. Lasonde: *Superalloys 718, 625, 706 and Various Derivatives*, ed. by E. A. Loria, (TMS, 1991) pp. 125–132.
- 3) N. K. Park, I. S. Kim, Y. S. Na and J. T. Yeom: *J. Mater. Process. Technol.* **111** (2001) 98–102.
- 4) D. E. Camus, R. A. Jaramillo, J. A. Plybum and F. S. Suarez: *Superalloys 718, 625, 706 and Various Derivatives*, ed. by E. A. Loria, (TMS, 1997) pp. 291–302.
- 5) L. X. Zhou and T. N. Baker: *Mater. Sci. Eng. A* **196** (1995) 89–95.
- 6) S. C. Medeiros, Y. V. R. K. Prasad, W. G. Frazier and R. Srinivasan: *Mater. Sci. Eng. A* **293** (2000) 198–207.
- 7) Y. S. Na, J. T. Yeom, N. K. Park and J. Y. Lee: *J. Mater. Process. Technol.* **141** (2003) 337–342.
- 8) Y. Wang, W. Z. Shao, L. Zhen, L. Lin and Y. X. Cui: *Mater. Sci. Forum* **546–549** (2007) 1297–1300.
- 9) J. W. Yoon, N. Y. Kim, J. H. Kim, J. T. Yeom and N. K. Park: *Key Eng. Mater.* **345–346** (2007) 57–60.
- 10) J. L. Russell, M. L. Lasonde and L. A. Jackman: *Superalloys 718, 625, 706 and Various Derivatives*, ed. by E. A. Loria, (TMS, 2005) pp. 363–372.
- 11) M. Donachie and S. Donachie: *Superalloys a Technical Guide*, (ASM International, 2003) pp. 91–108.
- 12) S. Mukhtarov, V. Valitov, M. F. X. Giglitti, P. R. Subramanian, J. S. Mate and N. Dudova: *Mater. Sci. Forum* **584–586** (2008) 458–463.
- 13) C. I. Garcia, G. D. Wang, D. E. Camus, E. A. Loria and A. J. DeArdo: *Superalloys 718, 625, 706 and Various Derivatives*, ed. by E. A. Loria, (TMS, 1994) pp. 293–302.
- 14) M. Sundararaman, P. Mukhopadhyay and S. Banerjee: *Metall. Trans. A* **19A** (1988) 453–465.
- 15) S. Azadian, L. Y. Wei and R. Warren: *Mater. Charact.* **53** (2004) 7–16.
- 16) V. Beaubois, J. Huez, S. Coste, O. Brucelle and J. Lacaze: *Mater. Sci. Technol.* **20** (2004) 1019–1026.
- 17) A. Thomas, M. El-Wahabi, J. M. Cabrera and J. M. Prado: *J. Mater. Process. Technol.* **177** (2006) 469–472.
- 18) W. C. Liu, F. R. Xiao and M. Yao: *Scr. Mater.* **37** (1997) 53–57.
- 19) M. Sundararaman, P. Mukhopadhyay and S. Banerjee: *Metall. Trans. A* **23A** (1992) 2015–2028.
- 20) S. J. Hong, W. P. Chen and T. W. Wang: *Metall. Mater. Trans. A* **32** (2001) 1887–1901.
- 21) C. T. Sims and W. C. Hagel: *The Superalloys*, (A Wiley Interscience Publication, 1972) pp. 134–137.
- 22) F. J. Humphreys and M. Hatherly: *Recrystallization and Related Annealing Phenomena*, (Elsevier Ltd, Oxford, 2004) pp. 285–293.
- 23) V. A. Phillips: *Trans. Metall. Soc. AIME* **236** (1966) 1302.
- 24) R. Li, M. Yao, W. Liu and X. He: *J. Mater. Eng. Perform.* **11** (2002) 504–508.
- 25) G. W. Han and Y. Y. Zhang: *Mater. Sci. Eng. A* **412** (2005) 198–203.
- 26) H. Y. Zhang, S. H. Zhang, M. Cheng and Z. X. Li: *Mater. Charact.* **61** (2010) 49–53.
- 27) M. Stockinger, E. Kozeschnik, B. Buchmayr and W. Horvath: *Superalloys 718, 625, 706 and Various Derivatives*, ed. by E. A. Loria, (TMS, 2001) pp. 141–148.